

## Investigating the role of hydrogen in indium oxide tubular nanostructures as a donor or oxygen vacancy passivation center

Mukesh Kumar, R. Chatterjee, S. Milikisiyants, A. Kanjilal, M. Voelskow, D. Grambole, K. V. Lakshmi, and J. P. Singh

Citation: [Applied Physics Letters](#) **95**, 013102 (2009); doi: 10.1063/1.3159786

View online: <http://dx.doi.org/10.1063/1.3159786>

View Table of Contents: <http://scitation.aip.org/content/aip/journal/apl/95/1?ver=pdfcov>

Published by the [AIP Publishing](#)

---

### Articles you may be interested in

[Investigation of defects in In–Ga–Zn oxide thin film using electron spin resonance signals](#)

J. Appl. Phys. **115**, 163707 (2014); 10.1063/1.4873638

[Depletion of nitrogenvacancy color centers in diamond via hydrogen passivation](#)

Appl. Phys. Lett. **100**, 071902 (2012); 10.1063/1.3684612

[Effective creation of oxygen vacancies as an electron carrier source in tin-doped indium oxide films by plasma sputtering](#)

J. Appl. Phys. **100**, 113701 (2006); 10.1063/1.2372571

[Indium oxide “rods in dots” nanostructures](#)

Appl. Phys. Lett. **89**, 063113 (2006); 10.1063/1.2335665

[Hydrogen passivation of nitrogen in 6H–SiC](#)

J. Appl. Phys. **82**, 6346 (1997); 10.1063/1.366525

---

An advertisement for Keysight B2980A Series Picoammeters/Electrometers. The ad features a red and white color scheme with a ruler graphic at the top. Text includes 'Confidently measure down to 0.01 fA and up to 10 PΩ' and 'Keysight B2980A Series Picoammeters/Electrometers'. A red button with white text says 'View video demo >'. An image of the device is shown next to the Keysight Technologies logo.

## Investigating the role of hydrogen in indium oxide tubular nanostructures as a donor or oxygen vacancy passivation center

Mukesh Kumar,<sup>1</sup> R. Chatterjee,<sup>2</sup> S. Milikisiyants,<sup>2</sup> A. Kanjilal,<sup>3</sup> M. Voelskow,<sup>3</sup> D. Grambole,<sup>3</sup> K. V. Lakshmi,<sup>2,a)</sup> and J. P. Singh<sup>1,a)</sup>

<sup>1</sup>Department of Physics, Indian Institute of Technology Delhi, Hauz Khas, New Delhi 110016, India

<sup>2</sup>Department of Chemistry and Chemical Biology and The Baruch '60 Center for Biochemical Solar Energy Research, Rensselaer Polytechnic Institute, 110 8th Street, Troy, New York 12180, USA

<sup>3</sup>Institute of Ion Beam Physics and Materials Research, Forschungszentrum Rossendorf, P.O. Box 510119, 01314 Dresden, Germany

(Received 20 March 2009; accepted 5 June 2009; published online 6 July 2009)

Electron paramagnetic resonance (EPR) spectroscopy of hydrogen-doped indium oxide (IO) tubular nanostructures shows presence of paramagnetic oxygen vacancies ( $V_O$ ) at room temperature. For temperatures below 80 K, the EPR spectra exhibit two distinct split resonances correspond to  $S = \frac{1}{2}$  hydrogen electron spin. Interestingly, presence of hydrogen EPR resonances is accompanied by absence of EPR signal of  $V_O$ , which is restored above 80 K with the concomitant disappearance of signature resonances from hydrogen. The temperature dependent donor and passivation behavior of hydrogen has been directly observed in metal oxide. This could provide valuable explanations of various  $V_O$  induced controversial properties of IO nanostructures. © 2009 American Institute of Physics. [DOI: 10.1063/1.3159786]

Hydrogen has attracted great attention as a source of secure, clean, sustainable energy, and it is environmentally benign as it does not generate greenhouse gases.<sup>1</sup> Hydrogen is ubiquitous and it is often difficult to remove hydrogen from synthesis of nanomaterials. Therefore, studying interaction of hydrogen with metals and semiconductors is of immense interest owing to the development of efficient materials for the storage of hydrogen and gas-sensing devices.<sup>2-7</sup> Ethanol has been suggested to be an efficient source of clean hydrogen.<sup>8,9</sup> The intentional (or unintentional) doping of materials with hydrogen exhibits qualitatively different behavior depending on the host matrix. Hydrogen can bind to the native defects and other impurities that are present in the host matrix and passivate their electrical activity. In contrast, bound hydrogen can also behave as a donor and increase the conductivity of the host matrix.<sup>6</sup> The interaction of hydrogen with transparent conducting oxides has always been important to tailor their electrical and optical properties.<sup>3,6,10,11</sup> High-mobility hydrogen-doped  $\text{In}_2\text{O}_3$  transparent conducting oxide has previously been reported for use in high efficiency  $a\text{-Si:H}/c\text{-Si}$  heterojunction solar cells.<sup>11</sup> Although, in most of the semiconductors hydrogen counteracts the prevailing conductivity, the incorporation of hydrogen in oxides, such as  $\text{In}_2\text{O}_3$  and  $\text{ZnO}$ , surprisingly results in donor activity ( $\text{H}^+$ ) and improves the electrical conductivity.<sup>3,6,12</sup> Hydrogen-doped indium oxide (IO) has been suggested as a better transparent conductor than the most commonly used tin-doped IO.<sup>3</sup> As a result, the unusual behavior of hydrogen in oxide matrices is of long standing interest to the scientific and engineering community. However, despite the importance and potential impact of IO on a large number of technological applications,<sup>3,11,13</sup> there exists a lack of experimental studies that detail the microscopic behavior of such systems.

In this letter, we study temperature dependent reversible switching behavior of hydrogen from donor ( $\text{H}^+$ ) to oxygen vacancy ( $V_O$ ) passivation center in hydrogen-doped IO tubular nanostructures (NS) using electron paramagnetic resonance (EPR) spectroscopy.

The hydrogen-doped IO tubular NS were synthesized by horizontal tube furnace maintained at a temperature of 1000 °C, one atmosphere pressure and constant flow of argon carrier gas at the rate of 200 mL/min for 1 h. An alumina boat with a 1:1 mixture of IO and active carbon powder was placed at the center of the tube furnace while silicon substrates were placed downstream at a temperature of 960 °C. A small reservoir (5–10 ml) of ethanol was placed in low temperature region ( $\sim 65$  °C) in upstream direction during the growth. Ethanol acts as the source of hydrogen. The high diffusion coefficient of hydrogen results in the incorporation of hydrogen in IO NS during the growth process.<sup>14</sup> The samples were characterized by glancing angle x-ray diffraction (GAXRD) and high-resolution transmission electron microscopy (HRTEM) (Tecnai G20-Stwin at 200 kV). The hydrogen content in IO tubular NS is measured at Rossendorf 5 MV tandem accelerator by resonant nuclear reaction analysis  $^{15}\text{N}(6.385 \text{ MeV}) + ^1\text{H} \rightarrow ^{12}\text{C} + ^4\text{He} + \gamma\text{-rays}(4.43 \text{ MeV})$ . The hydrogen depth profile is determined by gradually increasing the incident energy of  $^{15}\text{N}$  ions and thus moving the resonance at 6.385 MeV  $^{15}\text{N}$  ion energy progressively to greater depth.<sup>15</sup> The width of the resonance at 6.385 MeV is small enough to have a depth resolution of  $\sim 8$  nm. The EPR spectroscopy measurements were performed on a custom-built continuous wave (cw) X-band Eleksys 580 EPR spectrometer (Bruker BioSpin Corporation) operating at a frequency of 9.64 GHz and equipped with E-900 helium-flow cryostat (Oxford Instruments). The IO nanostructure samples were loaded into 4 mm quartz tubes and purged with argon gas prior to the EPR measurements. Typically, four scans were acquired for each spectrum under nonsaturating conditions at a microwave power of 3.13 mW. The spectra were acquired

<sup>a)</sup>Authors to whom correspondence should be addressed. Electronic addresses: lakshk@rpi.edu and jpsingh@physics.iitd.ac.in.

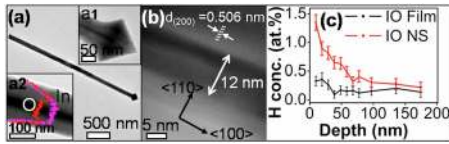


FIG. 1. (Color online) (a) TEM micrograph of a IO tubular NS. The inset a1 shows the HRTEM of tip region and reveals the presence of indium inside the cavity and inset a2 shows concentration profile of In and O along the radial direction of IO tubular structure along with STEM image. (b) HRTEM of tubular NS. (c) The hydrogen concentration (at. %) depth profile in IO tubular NS and IO thin film samples.

at a modulation frequency of 100 kHz with modulation amplitude of 1 G. The line shape of the cw EPR spectra of IO NS were simulated using *garlic* subroutine of the EASYSIM simulation program that uses an exact diagonalization approach.<sup>16</sup>

The GAXRD study (not shown here) of IO NS confirms the presence of cubic  $\text{In}_2\text{O}_3$  with a lattice constant  $a = 1.011$  nm. Figure 1(a) shows TEM micrograph of a tubular IO nanostructure with a typical diameter of 95 nm and an octahedral tip with a radius of curvature as low as 5 nm at the end. The cavity and wall thickness of various IO tubular NS vary from 10 to 60 nm and 35 to 100 nm, respectively. The HRTEM image of the tip region is shown as inset a1 of Fig. 1(a). The STEM-EDX measurement on IO tubular structure along its radial direction is shown in inset a2 of Fig. 1(a). The result confirms that the IO tubular NS are filled with indium metal. Figure 1(b) shows the lattice fringes of the two orthogonal planes of 0.506 and 0.71 nm which correspond to (200) and (110) planes of IO shell, respectively. The HRTEM micrographs reveal that the tubular NS grow along  $\langle 100 \rangle$  direction. The hydrogen concentration depth profiles for IO NS and IO thin film samples are shown in Fig. 1(c). The presence of hydrogen in IO NS sample is clearly seen in contrast to IO thin film. The measured concentration of hydrogen is found maximum at 10 nm below surface and then decreases rapidly toward the background level of IO thin film at the depth of  $\sim 170$  nm. The maximum hydrogen concentration is estimated to be  $\sim 10^{20} \text{ cm}^{-3}$ .<sup>15</sup>

Figures 2(a) and 2(b) show EPR spectroscopy results of IO tubular structures performed at a temperature range from 20 to 300 K. The EPR spectra at 20 K exhibit a sharp and intense hyperfine splitting due to the coupling of the electron spin ( $S = \frac{1}{2}$ ) with a nuclear spin ( $I = \frac{1}{2}$ ). The hyperfine coupling constant is 41.85 G (based on the separation of the EPR resonances and numerical simulations of the experimental EPR spectra). The doublet EPR signal is assigned to hydrogen hyperfine splitting ( $S = \frac{1}{2}$ ,  $I = \frac{1}{2}$ ). The EPR spectrum of

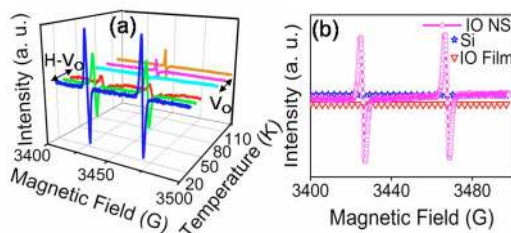


FIG. 2. (Color online) (a) The EPR spectra of IO tubular NS with temperature ranging from 20 to 120 K under nonsaturating conditions. (b) EPR spectra of IO tubular NS along with bare silicon substrate and indium oxide thin film deposited on silicon substrate.

hydrogen-doped diamondlike carbon films has previously been reported in literature and the two shoulders that are observed in the EPR spectrum were assigned to the presence of a hydrogen hyperfine splitting.<sup>17</sup> Similar results have also been reported for hydrogen in ZnO at 5 K. Although the hyperfine splitting was not resolved in the hydrogen spectrum from ZnO and electron-nuclear double resonance spectroscopy was used to identify the chemical nature of hydrogen spin.<sup>12</sup> The two sharp intense peaks that result from a hyperfine coupled hydrogen spin in the present study arise from simultaneous microwave-induced spin flips of the electron spin ( $S = \frac{1}{2}$ ) as reported in hydrogen-doped diamond thin film. The simulation of the hyperfine coupled EPR spectrum of hydrogen-doped IO NS reveals that the  $g$  value, hyperfine coupling constant and line width for the numerical simulations that best reproduce the experimental EPR spectra are 1.9991, 116.75 MHz, and 0.28 G, respectively. As the temperature is increased from 20 to 40 K, the intensity of the hyperfine coupled EPR signal decreases. The hyperfine coupled EPR signal completely disappears at 80 K with the appearance of a new peak that arises at 3445.6 G, in the  $g \sim 2$  region of the EPR spectrum, as shown in Fig. 2(a). The intensity of the 3445.6 G peak increases as the temperature is raised from 80 to 300 K (EPR spectrum at 300 K is not included in the figure). Numerical spectral simulations of single EPR signal at 3445.6 G indicate  $g$  value of 2.0025, which is in close agreement with the reported  $g$  value for the native oxygen vacancy defect in IO.<sup>18-20</sup> To confirm that the hydrogen signal arises from the IO tubular NS, EPR measurements were conducted on the control samples of the Si substrate and IO thin film on Si substrate at 20 K as shown in Fig. 2(b). The IO thin film is deposited by thermal evaporation on silicon substrate and this procedure is followed by air annealing at 960 °C in the absence of ethanol. It is important to note that we do not detect an EPR signal for the substrate in the absence and the presence of IO thin films on the silicon substrate. This confirms that the hyperfine coupled EPR spectra for IO tubular NS arise from the presence of hydrogen defects. We have also performed EPR spectroscopy measurements on the base cavity at 20 K. Once again, hyperfine coupled EPR signals are not detected in the samples of the base cavity. These observations clearly reveal that the hydrogen is present only within the IO NS and does not arise from the substrate.

To understand the temperature dependence of the EPR spectra that are obtained from IO NS, we discuss the charge interaction between doped hydrogen and oxygen vacancies in IO matrix. de Walle and Neugebauer<sup>6</sup> have proposed a generalized theory on the basis of electronic transition level of hydrogen in semiconductors, insulators and solutions. Within this picture, the electronic transition level,  $\epsilon(+/-)$ , allows the prediction of electrical activity of hydrogen, which acts either as a donor ( $\text{H}^+$ ) or an acceptor ( $\text{H}^-$ ) in any matrix. In any semiconductor that has  $\epsilon(+/-)$  level above the conduction band minima, hydrogen behaves as donor ( $\text{H}^+$ ) for any value of Fermi energy. The ZnO,  $\text{In}_2\text{O}_3$ , and InN materials are included in this category and hydrogen behaves as a donor and increases the electrical conductivity of these materials.<sup>3,6,21</sup> Figure 3(a) shows the position of  $\epsilon(+/-)$  level in the conduction band that reveals the donor ( $\text{H}^+$ ) nature of hydrogen in IO. In addition,  $\text{H}^+$  could interact with different native defects that are present in IO matrix. The possible



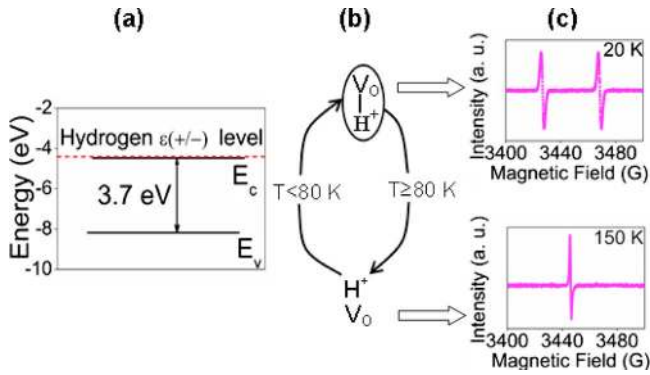


FIG. 3. (Color online) (a) Illustration of hydrogen energy level,  $\epsilon(+/-)$ , with respect to valance band maxima for IO. The presence of  $\epsilon(+/-)$  energy level in conduction band indicates the donor nature of hydrogen. (b) A depiction of temperature dependent interaction of donor hydrogen with singly charged oxygen vacancy. (c) EPR spectra of IO tubular NS at 20 and 150 K which correspond to the presence of hydrogen hyperfine coupled spins and the oxygen vacancies, respectively.

defects in IO are oxygen vacancy ( $V_O$ ), oxygen antisite ( $O_{In}$ ), oxygen interstitial ( $O_i$ ), indium interstitial ( $In_i$ ), indium vacancies ( $V_{In}$ ) and their complexes. The large diameter of the oxygen atom (1.38 Å) with respect to the cell volume reduces the possibility of forming  $O_i$  defects. Also, despite the large number of possible defects in the IO matrix,  $In_i$  and  $V_O$  have been reported as the dominant defects.<sup>22,23</sup> The interaction of hydrogen with  $In_i$  seems unlikely as it has been reported that indium hydride is very unstable due to the instability of In–H bond. It is only possible to stabilize monomeric  $InH_3$  in a solid argon matrix at 10 K.<sup>24</sup> In the present study, the temperature dependent EPR [Fig. 2(a)] suggest that the doped hydrogen interacts with the IO matrix even at 40 K and clearly displays the corresponding hyperfine coupled EPR resonances. The indium interstitials remain in the triplet charge state ( $In_i^{3+}$ ) in IO and it is interesting to note that  $In_i^{3+}$  ( $[Kr]4d^{10}$ ) is diamagnetic in nature.<sup>23</sup> Hence,  $In_i^{3+}$  does not display an EPR signal. We propose that the doped hydrogen may have tendency to interact with  $V_O$  in IO matrix and form a complex defect ( $H^+-V_O$ ) that effectively behaves as hydrogen atom. The EPR spectroscopic measurement on the IO tubular nanostructure at 20 K exhibits a typical hydrogen hyperfine splitting and confirms this hypothesis. Also, the measured concentration of hydrogen ( $10^{20} \text{ cm}^{-3}$ ) is in close agreement with the concentration of oxygen vacancies reported in literature.<sup>25</sup> So, at 20 K hydrogen passivate almost all the oxygen vacancies present in IO NS. With the increase in temperature, thermal energy weakens the  $H^+-V_O$  interaction. This leads to a decrease in the intensity of hydrogen EPR signal. For temperatures above 80 K, the complex defect ( $H^+-V_O$ ) dissociates into  $H^+$  and  $V_O$ , which results in a single EPR peak corresponding to  $V_O$ , as  $H^+$  is not paramagnetic in nature. The temperature dependent interaction between  $H^+$  and  $V_O$  and the corresponding EPR spectra are shown in Figs. 3(b) and 3(c), respectively. The interaction strength between  $H^+$  and  $V_O$  is determined on the basis of the temperature (80 K) and is found to be 7 meV. A

similar thermal activation energy of  $4 \pm 2$  meV is reported for H to release an electron to the conduction band in a ZnO matrix.<sup>12</sup>

In summary, a temperature dependent reversible switching behavior of hydrogen from electrical donor to oxygen vacancy passivation was studied in hydrogen-doped IO tubular NS by variable temperature EPR spectroscopy. The doped hydrogen which usually acts as donor at room temperature is found to interact with  $V_O$  below 80 K and forms a paramagnetic complex defect ( $H^+-V_O$ ). The unusual  $V_O$  passivation by doped hydrogen at low temperature ( $<80$  K) will greatly impact many unresolved  $V_O$ -dependent physical properties of IO such as photoluminescence and ferromagnetism that remain elusive at present.<sup>18–20,26</sup>

- <sup>1</sup>G. A. Deluga, J. R. Salge, L. D. Schmidt, and X. E. Verykios, *Science* **303**, 993 (2004).
- <sup>2</sup>I. Aruna, B. R. Mehta, L. K. Malhotra, and S. M. Shivaprasad, *Adv. Mater. (Weinheim, Ger.)* **16**, 169 (2004).
- <sup>3</sup>T. Koida, H. Fujiwara, and M. Kondo, *Jpn. J. Appl. Phys., Part 2* **46**, L685 (2007).
- <sup>4</sup>D. C. Elias, R. R. Nair, T. M. G. Mohiuddin, S. V. Morozov, P. Blake, M. P. Halsall, A. C. Ferrari, D. W. Boukvalov, M. I. Katsnelson, A. K. Geim, and K. S. Novoselov, *Science* **323**, 610 (2009).
- <sup>5</sup>L. Schlapbach and A. Züttel, *Nature (London)* **414**, 353 (2001).
- <sup>6</sup>C. G. Van de Walle and J. Neugebauer, *Nature (London)* **423**, 626 (2003).
- <sup>7</sup>T. Xu, M. P. Zach, Z. L. Xiao, D. Rosenmann, U. Welp, W. K. Kwok, and G. W. Crabtree, *Appl. Phys. Lett.* **86**, 203104 (2005).
- <sup>8</sup>A. Kowal, M. Li, M. Shao, K. Sasaki, M. B. Vukmirovic, J. Zhang, N. S. Marinkovic, P. Liu, A. I. Frenkel, and R. R. Adzic, *Nature Mater.* **8**, 325 (2009).
- <sup>9</sup>K. Otsuka, A. Mito, S. Takenaka, and I. Yamanaka, *Int. J. Hydrogen Energy* **26**, 191 (2001).
- <sup>10</sup>T. Koida, H. Fujiwara, and M. Kondo, *Sol. Energy Mater. Sol. Cells* **93**, 851 (2009).
- <sup>11</sup>N. Ohashi, T. Ishigaki, N. Okada, T. Sekiguchi, I. Sakaguchi, and H. Haneda, *Appl. Phys. Lett.* **80**, 2869 (2002).
- <sup>12</sup>D. M. Hofmann, A. Hofstaetter, F. Leiter, H. Zhou, F. Henecker, B. K. Meyer, S. B. Orlinskii, J. Schmidt, and P. G. Baranov, *Phys. Rev. Lett.* **88**, 045504 (2002).
- <sup>13</sup>C. Li, W. Fan, B. Lei, D. Zhang, S. Han, T. Tang, X. Liu, Z. Liu, S. Asano, M. Li, W. Yappan, J. Han, and C. Zhou, *Appl. Phys. Lett.* **84**, 1949 (2004).
- <sup>14</sup>R. Schiller, G. Battistig, and J. Rabani, *Radiat. Phys. Chem.* **72**, 217 (2005).
- <sup>15</sup>M. H. Brodsky, M. A. Frisch, J. F. Ziegler, and W. A. Lanford, *Appl. Phys. Lett.* **30**, 561 (1977).
- <sup>16</sup>S. Stoll and A. Schweiger, *J. Magn. Reson.* **178**, 42 (2006).
- <sup>17</sup>S. L. Holder, L. G. Rowan, and J. J. Krebs, *Appl. Phys. Lett.* **64**, 1091 (1994).
- <sup>18</sup>M. Kumar, V. N. Singh, F. Singh, K. V. Lakshmi, B. R. Mehta, and J. P. Singh, *Appl. Phys. Lett.* **92**, 171907 (2008).
- <sup>19</sup>P. Guha, S. Kar, and S. Chaudhuri, *Appl. Phys. Lett.* **85**, 3851 (2004).
- <sup>20</sup>M. J. Zheng, L. D. Zhang, G. H. Li, X. Y. Zhang, and X. F. Wang, *Appl. Phys. Lett.* **79**, 839 (2001).
- <sup>21</sup>E. A. Davis, S. F. J. Cox, R. L. Lichti, and V. G. Van de Walle, *Appl. Phys. Lett.* **82**, 592 (2003).
- <sup>22</sup>T. Tomita, K. Yamashita, and Y. Hayafuji, *Appl. Phys. Lett.* **87**, 051911 (2005).
- <sup>23</sup>J. H. W. De Wit, *J. Solid State Chem.* **8**, 142 (1973).
- <sup>24</sup>P. Pullumbi, Y. Bouteiller, L. Manceron, and C. Mijoule, *Chem. Phys.* **185**, 25 (1994).
- <sup>25</sup>J. R. Bellingham, A. P. Mackenzie, and W. A. Phillips, *Appl. Phys. Lett.* **58**, 2506 (1991).
- <sup>26</sup>A. Sundaresan, R. Bhargavi, N. Rangarajan, U. Siddesh, and C. N. R. Rao, *Phys. Rev. B* **74**, 161306(R) (2006).